

## Turbulence and Diffusion: Fossil Turbulence (MS 138)

Carl H. Gibson, Professor of Engineering Physics and Oceanography  
 Departments of MAE and Scripps Institution of Oceanography  
 University of California at San Diego, La Jolla, CA 92093-0411  
 cgibson@ucsd.edu, <http://www-ac.scs.ucsd.edu/~ir118>

### Introduction

Fossil turbulence processes are central to turbulence, turbulent mixing, and turbulent diffusion in the ocean and atmosphere, in astrophysics and cosmology, and in most other natural flows. George Gamov suggested in 1954 that galaxies might be fossils of primordial turbulence produced by the Big Bang. John Woods showed that breaking internal waves on horizontal dye sheets in the interior of the stratified ocean form highly persistent remnants of these turbulent events, which he called fossil turbulence. Woods organized a fossil turbulence workshop in 1969 to synthesize similar observations of turbulence "footprints" in other stratified atmospheric and oceanic regions; in particular, persistent anisotropic patches of refractive index detected by radio wave scattering far downstream of mountains, and patches of strong temperature microstructure without strong velocity fluctuations detected from submarines by Robert Stewart and Pat Nasmyth. A universal similarity theory of stratified fossil turbulence presented by Gibson in 1980 estimated universal constants of stratified fossil turbulence and introduced hydrodynamic phase diagrams as a method for classifying temperature and salinity microstructure patches in the ocean interior according to their hydrodynamic states (turbulent, active-fossil turbulence, completely fossil), and for extracting fossilized information about the previous turbulence and mixing. The theory is confirmed by measurements of Lozovatsky, Dillon, Gargett, Gregg, Osborne, Van Atta and others, and has been extended to describe fossilized turbulence constrained by Coriolis forces, self-gravitational forces, and magnetic forces.

Turbulence always forms first at the smallest length scale permitted by viscous forces; that is, the Kolmogorov scale  $L_K$ . Turbulence then cascades by a sequence of eddy pairings, pairings of eddy pairs, and so forth to larger and larger scales, extracting energy from non-turbulent ambient shears and waves by inertial-vortex forces  $\vec{v} \times \vec{\omega}$ , where  $\vec{v}$  is the velocity field and  $\vec{\omega}$  is the vorticity field  $\nabla \times \vec{v}$ . A common misconception is that turbulence cascades from large scales to small. This ancient myth, canonized by Richardson's poem, gives the direction of the non-turbulent energy cascade. The non-turbulent cascade is induced by the inertial-vortex forces of the turbulence as it entrains large scale irrotational non-turbulent fluid which becomes turbulent at the viscous scale  $L_K$  when it becomes rotational. Vertical buoyancy forces and horizontal Coriolis forces of the stratified, rotating, ocean eventually constrain the inertial-vortex forces of turbulence patches formed in the ocean interior and convert the turbulence to patches of non-propagating, partially turbulent, persistent waves that are termed fossil-vorticity-turbulence and have often been mistaken for turbulence in oceanic turbulence sampling experiments that fail to account for the turbulent

fossilization process. Such mistakes have led to vast underestimates of the true average vertical turbulence flux rates, and are the source of the so-called "deep dark mixing" paradox of the deep ocean interior (a concept invented by Tom Dillon). Deep dark mixing is to the ocean as dark matter is to galaxies. Dark matter is unseen matter that must exist to prevent galaxies from flying apart by centrifugal forces. Dark mixing is mixing by turbulence events that must exist to explain why the deep ocean interior is well mixed, but which is undetected except for the fossil turbulence remnants. Fossil-vorticity-turbulence motions represent unique classes of saturated, nonlinear, internal and inertial waves that can only be naturally produced by damping turbulence. Scalar fields like temperature, salinity, and nutrient concentrations are mixed and diffused in the ocean by a complex amalgam of turbulence and fossil-vorticity-turbulence.

Fossil-scalar-turbulence signatures preserve information about previous turbulence; for example, temperature fluctuations produced by turbulence for fluctuations at length scales where the turbulence has been damped by buoyancy are termed fossil-temperature-turbulence, just as skywriting rapidly becomes fossil-smoke-turbulence above the inversion layer. The larger the fossil temperature turbulence patch, the larger the viscous and temperature dissipation rates must have been in the original patch of turbulence. Fossil turbulence remnants are the footprints and scars of previous turbulent events, and preserve information about their origins in a wide variety of hydrophysical fields of the ocean. The process of extracting information about previous turbulence and mixing from fossil turbulence is termed hydropaleontology.

Stratified and rotating fossils of turbulence are more persistent than their progenitor turbulence events because they possess almost the same velocity variance (kinetic energy) and scalar variance (potential entropy of mixing) as the original turbulent field, but have smaller viscous and scalar dissipation rates of these quantities than they had while they were fully turbulent. The most powerful turbulence events produce the most persistent fossils, with persistence times proportional to the normalized Reynolds number and inversely proportional to the stratification frequency. Oceanic fossil turbulence processes are more complex and important than fossil turbulence in non-stratified non-rotating flows where the only mechanism of fossilization is the viscous damping of turbulence before mixing is complete. Laboratory viscous fossil turbulence without stratification or rotation is thus mentioned in textbooks only as a curiosity of flow visualization, where eddy patterns of dye or smoke that appear to be turbulent are not because the turbulent fluid motions have been damped by viscosity.

Most of the ocean's kinetic energy exists as fossil-vorticity-turbulence because its motions, both from air-sea interaction and gravitational forces of the sun and moon, are converted to turbulence energy at the top and bottom ocean surfaces by turbulent friction and not immediately or locally dissipated but fossilized by buoyancy and Coriolis forces and distributed oceanwide by advection as they slowly decay, leaving fossil-scalar-turbulence and fossil-vorticity-turbulence remnants in a variety of hydrodynamic states. These turbulence fossils move and interact with their environment and each other in the ocean interior by mechanisms that are sometimes poorly understood and hardly recognized. For example, a necessary stage of double diffusive vertical fluxes in the ocean may be in the

final stages of fossil-temperature-salinity-turbulence decay. The turbulence event scrambles the temperature and salinity fields to produce the full range of possible double diffusive instabilities which function in the late stages of the turbulent fossil decay, leaving characteristic layered structures of salt fingering. Powerful turbulence events produce fossils that decay by turbulence formation, this turbulence fossilizes, and these fossils produce more turbulence. Turbulent mixing and diffusion is initiated by turbulence, but the final stages of the mixing and diffusion is completed only after the flow has become partially or completely fossilized.

## History of fossil turbulence

The distinctive, eddy-like-patterns of turbulent motions are beautiful and easily recognized. Many ancient civilizations have woven them into their arts, religions and sciences. The first attempts at hydropaleontology were applications of Kolmogorovian universal similarity theories of turbulence to cosmology by Gamov, Zel'dovich, Ozernoi and others of the Soviet school of turbulence. These attempts ceased in the 1970s because measurements of the cosmic microwave background temperature  $T$  showed  $T/T$  fluctuations were only  $10^{-5}$ . Such small  $T/T$  values prove the primordial universe was not strongly turbulent since unconstrained turbulence would produce  $T/T = 10^{-2}$ . However, recent applications of hydropaleontology to better astrophysical observations from the Hubble Space Telescope and a variety of other modern instruments confirm Gamov's speculation that astrophysical and cosmological structures are hydrodynamic fossils, with fossils of non-turbulence as well as turbulence. Viscous as well as turbulence forces determined the primordial masses of fragmentation and condensation by self-gravitation, leading to present structures like superclusters, galaxies, stars, and forms of the dark matter. Information about ancient and primordial hydrodynamic states is preserved by these fossils.

Woods' 1969 Radio Science fossil turbulence workshop examined patches of persistent refractive index fluctuations produced by turbulence in the stratified atmosphere and fluctuating temperature and dye patches produced by turbulence in the ocean interior which could not possibly be turbulent at the time of their detection. Woods and other scuba divers observed dye patch fossils of breaking internal waves from their turbulent beginning until they became motionless. Stewart reported temperature microstructure patches from a submarine with and without measurable velocity fluctuations, indicating that those without must be fossilized. Fossil turbulence patches produced in the stratified atmosphere by wind over mountains and wakes of other aircraft are dangerous to aircraft because of the long persistence times of stratified fossil vorticity turbulence patches. Detectable refractive index fluctuations from billow turbulence events behind mountains are observed many miles downstream by radar scattering measurements, long after all turbulence had been damped by buoyancy forces as shown by the layered anisotropy that develops in the radar returns reported in the Woods workshop. Similar patches at high altitudes, apparently fossils of clear air turbulence, are well known to radar operators and referred to as "angels". Such a fossil turbulence patch sent passengers flying into the ceiling of a Boeing 737 at 24,000 feet the afternoon of September 3, 1999, bound from Los Angeles to San Francisco on United Flight 2036, injuring 15 of the 107 passengers and five crew aboard.

A quantitative universal similarity theory of stratified fossil turbulence was published by Gibson in 1980 based on towed-body small-scale temperature measurements made in 1974 with John Schedvin in the upper ocean of the Flinders current off Australia in a US-Soviet intercomparison cruise with R. Ozmidov, V. Paka, I. Lozovatzky and V. Nabatov on the DMITRI MENDELEEV. The data showed clear evidence of buoyancy effects causing departures from spectral forms of the Kolmogorov and Batchelor universal similarity theories of turbulence and turbulent mixing. These were attributed to stratified turbulence fossilization. The theory is illustrated by the velocity and temperature dissipation spectra expected for five stages of a buoyancy fossilized turbulent wake in Figure 1.

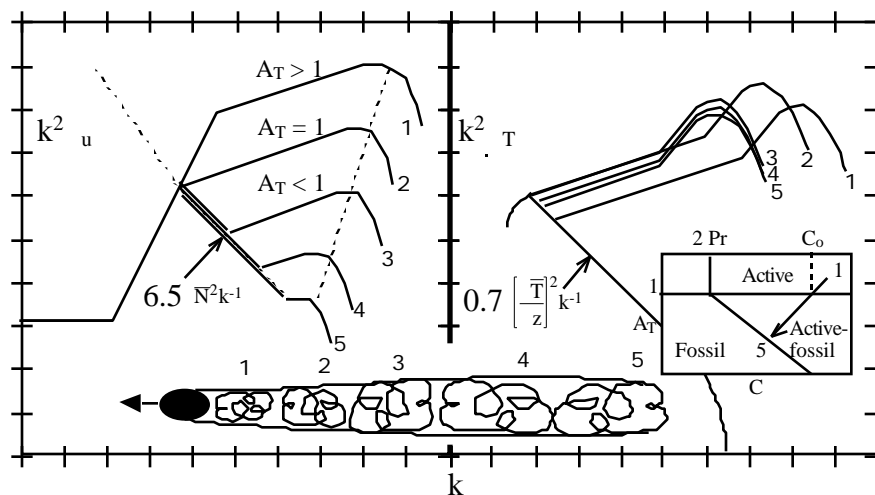


**Figure 1.** Dissipation spectra for velocity, left, and temperature, right, for active turbulence as it fossilizes, represented by five stages of a temperature stratified turbulent wake in water, bottom (from Gibson 1999). Universal spectral forms for the saturated internal waves of the remnant fossil-vorticity-turbulence and fossil-temperature-turbulence microstructure patch are from Gibson (1980). The trajectory on an  $A_T$  versus  $C$  hydrodynamic phase diagram is shown in the right insert.

Stage 1 of the turbulence patch is fully turbulent, and the viscous dissipation rate spectrum  $k^2_u$  shown on the left of Fig. 1, with area  $\propto k^{-3}$  and slope  $+1/3$  according to Kolmogorov's second hypothesis for wavenumbers  $k \propto 2\pi/L$  between the energy (or Obukhov) scale  $L_0$  on the left and the Kolmogorov scale  $L_K$  on the right. The turbulence continues its cascade to larger  $L_0$  scales by entrainment of external non-turbulent fluid until the increasing  $L_0$  is matched by the decreasing Ozmidov scale  $L_R = (\epsilon/N^3)^{1/2}$  at the beginning of fossilization, where  $\epsilon = \epsilon_0$ , with spectral forms 2. The temperature dissipation spectrum  $k^2_T$  increases in amplitude from stage 1 to 2 as vertical temperature differences are entrained over larger vertical scales, even though the velocity spectrum  $k^2_u$  decreases, with increasing area  $\epsilon/\epsilon_0 = C(\bar{T}/z)^2/3$ , where  $\epsilon$  is the diffusive dissipation rate of temperature variance and Cox number  $C$  is the mean square over square mean temperature

gradient ratio. The dramatic differences in spectral shapes between the velocity dissipation spectra and the temperature dissipation spectra in Fig. 1 reflects the fact that the kinetic energy of the fossilized turbulence event persists in the fossil-vorticity-turbulence for much longer periods than the temperature variance persists in the fossil-temperature-turbulence. This is the basis of the  $A_T (\epsilon / \rho)^{1/2}$  versus  $C$  hydrodynamic phase diagram shown at the bottom right of Fig. 1. Because  $\epsilon$  and  $C$  are large in the temperature fossil, the velocity dissipation rate at beginning of fossilization  $\epsilon_0$  can be estimated from  $\epsilon_0 = 13DCN^2$  from the Gibson 1980 theory. The turbulent activity coefficient  $A_T (\epsilon / \rho)^{1/2}$  is greater than 1 for stratified turbulence patches before fossilization, and less than 1 after fossilization begins. A particular patch decays along a straight line trajectory in the HPD until  $\epsilon = \epsilon_F = 30 N^2$  at complete fossilization. It can be shown that  $C$  averaged over a large horizontal layer in the stratified ocean for a long time period is a good measure of the turbulent heat flux divided by the molecular heat flux (Osborne and Cox 1972), with the vertical turbulent diffusivity  $K = DC$ . The motivation for most oceanic microstructure measurements is to estimate  $K$  through measurements of the average  $C$  for various oceanic layers. The problem is that  $C$ ,  $\epsilon$ , and  $N$  in the ocean, atmosphere and all other natural fluids tend to be extremely intermittent.

## Intermittency of oceanic turbulence and mixing

Turbulence at the enormous Reynolds numbers of oceanic and atmospheric turbulence is notoriously intermittent in space and time. Sampling turbulence and turbulent mixing in the ocean without recognizing this intermittency and without recognizing that most oceanic microstructure in the ocean is fossilized or partially fossilized has led to misinterpretations and vast errors in estimates of turbulent diffusion and mixing rates from measured microstructure data in the ocean interior. As mentioned, the dark mixing paradox of the ocean refers to undetected mixing that must exist somewhere to explain why oceanic scalar fields like temperature and salinity are so well mixed, just as the dark matter paradox of galaxies refers to undetected matter that must exist to explain why rotating galaxies don't fly apart by centrifugal forces. Both paradoxes result from sampling techniques that fail to account for the extreme intermittency of oceanic turbulent mixing and self-gravitating galactic mass density, which are both random variables involved in self-similar, nonlinear, cascades over a wide range of scales.

In galaxies, the nonlinear cascade is gravitational condensation and the intermittent random variable is the number density  $n$  of the dark matter objects. The galactic dark matter is revealed to be Earth-mass rogue planets (many millions for every star) by quasar microlensing that averages the total mass of the lens galaxy to produce twinkling images of the background quasar. The twinkling frequency gives the mass of the point mass objects dominating the lens galaxy mass (Schild 1996). These primordial hydrogenous-planetoids (Neptunes) are effectively undetectable by star-microlensing studies that assume  $n$  is constant, even though millions of stars have been used for recent MACHO (massive astrophysical compact halo object) searches for dark matter in the Milky Way halo. The dark-matter planets ( $10^{17}$  per galaxy) are sequestered in clumps and clusters by their nonlinear accretional cascade to form stars, just as the dominant mixing patches of the ocean

interior escape detection by dropsonde-sampling because the extreme intermittency of oceanic turbulence mixing causes them to clump and cluster in both space and time.

In the ocean the nonlinear cascade is that of the vorticity in turbulence and turbulent mixing, and the intermittent random variables are  $C$ , the temperature and viscous dissipation rates  $\epsilon$  and  $\chi$ , and various turbulent diffusivities that can be derived from average values of these quantities. The random variables  $n$ ,  $\epsilon$ , and  $\chi$  in these examples have extremely intermittent lognormal distribution functions, with mean values much larger than mode values. Turbulent diffusivities are proportional to mean values of  $\epsilon$  and  $\chi$ , so it is crucial to know the mean/mode ratios of the random variables, termed the Gurvich numbers  $G$ , to be able to correct average values from small data sets that assume  $\epsilon$  and  $\chi$  are uniformly distributed. For lognormal random variables,  $G_X = \exp[3 \sigma_{\ln X}^2/2]$ , where  $\sigma_{\ln X}^2$  is the variance or intermittency factor of a lognormal random variable  $X$ . Intermittency factors  $\sigma_{\ln \epsilon}^2$  and  $\sigma_{\ln \chi}^2$  in the ocean have been measured, and range from typical values of 5 at midlatitudes near the surface, to 6 or 7 in the deep ocean and at equatorial latitudes. Thus, probable undersampling errors for these quantities range from  $G_\epsilon = 1800$  to 36,000 in the ocean.  $G_n$  values are likely to be even larger, of order  $10^6$ . For comparison, the intermittency factor  $\sigma_{\ln \$}^2$  of the super-rich (upper 3%) US personal income, which is close to lognormal, has been measured to be 4.3, giving a Gurvich number  $G_\$$  of 600. Figure 2 shows a lognormality plot of independent deep ocean samples of  $X = C$  averaged over 150 meters in the vertical. The axes are stretched so lognormal random variables fit a straight line.

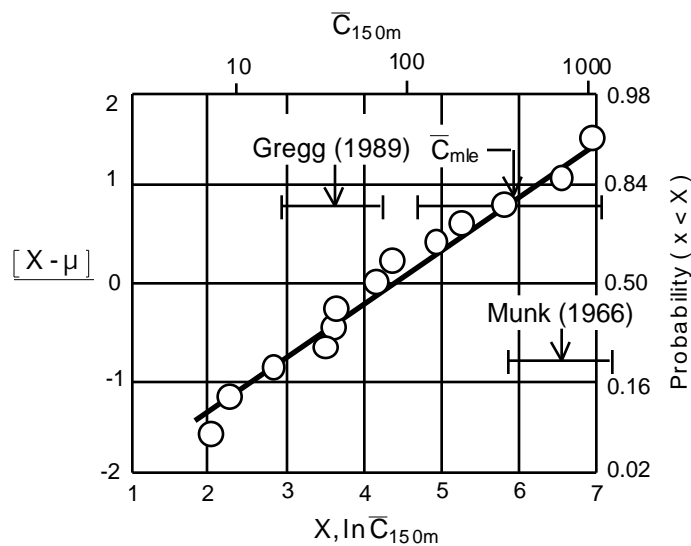


**Figure 2.** Normalized lognormal probability plot of dropsonde Cox number samples, averaged over 150 m in the vertical, in the depth range 75-1196 m, from Gregg (1977), expedition Tasaday 11, February, 1974. Estimated 95% confidence intervals are shown by horizontal bars, and compared to confidence intervals for  $C$  from the Gregg (1989) and Munk (1966) models for the thermocline.

Fig. 2 (from Gibson 1991) shows the effects of undersampling errors due to intermittency in attempts to estimate the Cox number  $C$  of the stratified layers of the deep ocean, illustrating the deep dark mixing paradox. Munk 1966 published a classic "Abyssal Recipe" paper estimating the vertical turbulent diffusivity of temperature in the deep Pacific Ocean below a kilometer depth should be about  $K = DC = 1\text{--}2 \text{ cm}^2 \text{ s}^{-1}$  (this cgs unit is often termed one "Munk") with corresponding Cox number of 500–1100. Based on dropsonde temperature microstructure measurements, Gregg 1989 claims values more than an order of magnitude less. However, Gregg's deep  $C$  averages are clearly lognormal, with maximum likelihood estimator  $C_{\text{mle}}$  values in better agreement with the Munk range than with the Gregg range, as shown in Fig. 2. This matter is still controversial in the oceanographic literature.

## Turbulence and fossil turbulence definitions

Turbulence is defined as an eddy-like state of fluid motion where the inertial-vortex forces of the eddies are larger than any of the other forces which tend to damp the eddies out. The inertial-vortex force  $\vec{F}_I = \vec{v} \times \vec{\omega}$  produces turbulence, and appears in the Newtonian momentum conservation equations,

$$\frac{d\vec{v}}{dt} = -\vec{B} + \vec{v} \times \vec{\omega} + \vec{F} + \vec{F}_C + \vec{F}_B + \dots; \quad B = \frac{p}{\rho} + \frac{v^2}{2} + gz, \quad (1)$$

where  $\vec{v}$  is the velocity field,  $\vec{\omega} = \nabla \times \vec{v}$  is the vorticity,  $B$  is the Bernoulli group of mechanical energy terms,  $p$  is pressure,  $\rho$  is density,  $g$  is gravity,  $z$  is up,  $\vec{F} = \mu \nabla^2 \vec{v}$  is the viscous force (per unit mass),  $\mu$  is the kinematic viscosity,  $\vec{F}_C = 2\vec{v} \times \vec{\omega}$  is the Coriolis force, and  $\vec{F}_B = N^2 L$  is the buoyancy force when the stratification frequency  $N$  is averaged over the largest vertical scale  $L$  of the turbulence event (other forces are neglected). The growth of turbulence is driven by  $\vec{F}_I$  forces at all scales of the turbulent fluid. Irrotational flows with  $\vec{\omega} = 0$  are nonturbulent by definition, but supply the kinetic energy of turbulence because the turbulent fluid induces a nonturbulent cascade of the irrotational fluid from large to small scales. In turbulent flows, viscous and inertial-vortex forces are equal at a universal critical Reynolds number  $v x / \mu \approx 100$  for separation distances  $x \approx 10 L_K$ , where  $L_K$  is the Kolmogorov length scale

$$L_K = \left[ \frac{\epsilon}{3} \right]^{1/4} \quad (2)$$

and  $\epsilon$  is the viscous dissipation rate per unit mass.

Fossil turbulence is defined as a fluctuation in any hydrophysical field produced by turbulence that persists after the fluid is no longer turbulent at the scale of the fluctuation. Examples of fossil turbulence are jet contrails, skywriting, remnants of cold milk poured rapidly into hot coffee, and patches of ocean temperature microstructure observed with little or no velocity microstructure existing within the patches. The best known fossil turbulence in the ocean is the mixed layer depth, which persists long after it was produced. Buoyancy forces match inertial-vortex forces in a turbulent flow at the Ozmidov scale

$$L_R = \left[ \frac{g}{N^3} \right]^{1/2}, \quad (3)$$

where the intrinsic frequency  $N$  of a stratified fluid is

$$N = \left[ \frac{g}{z} \right]^{1/2}, \quad (4)$$

for the ambient stably stratified fluid affecting the turbulence. Coriolis forces match inertial-vortex forces at the Hopfinger scale

$$L_H = \left[ \frac{g}{3} \right]^{1/4}, \quad (5)$$

where  $\Omega$  is the angular velocity of the rotating coordinate system.

Taking the curl of Equation (1) for a stratified fluid gives the vorticity conservation equation

$$\frac{d\vec{\omega}}{dt} + \vec{\nabla} \cdot \vec{\omega} = \vec{\nabla} \times \vec{\omega} + \frac{\nabla \times \mathbf{p}}{2} + \nu \nabla^2 \vec{\omega}, \quad (6)$$

where the vorticity of fluid particles (on the left side) tends to increase from vortex line stretching by the rate of strain tensor  $\vec{\nabla} \cdot \vec{\omega}$  (the first term on the right), baroclinic torques on strongly tilted strong density gradient surfaces (the second term), and decreases by viscous diffusion (the third term). From Equation (6) we see that turbulence events in stably stratified natural fluids are most likely to occur where the stratification is maximum for long time periods; for example on fronts, because this is where most of the vorticity is produced, but this is also where the turbulence is most strongly inhibited.

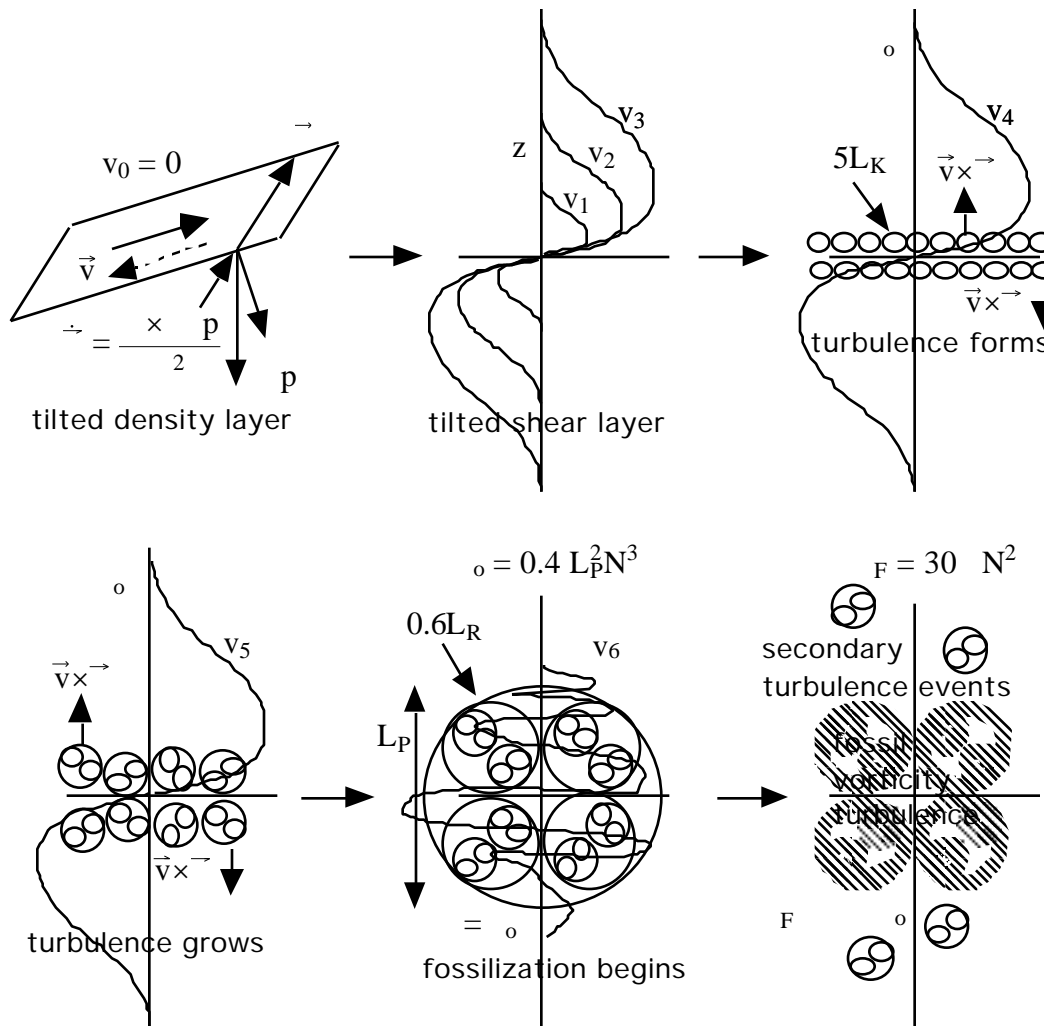
## Formation and detection of stratified fossil turbulence

Figure 3 shows a typical sequence of events for turbulence and fossil turbulence formation in the interior of the stratified ocean where vorticity is produced by density surface tilting rather than shear on a solid surface. The longer the density surface is tilted the more kinetic energy is stored in the resulting boundary layers. The boundary layers formed on both sides of the tilted surface will become turbulent when a critical Reynolds number is reached. This occurs when the boundary layer thickness is 5-10 Kolmogorov scales based on the viscous dissipation rate of the laminar boundary layer. The eddies pair, and the pairs of eddies pair with pairs of eddies, etc., as shown bottom left and center of Fig. 3. Fossilization begins when buoyancy forces match the inertial vortex forces of the turbulence, at a vertical size of about  $0.6 L_R$ , as shown at bottom center. The dissipation rate monotonically decreases with time during the process so  $L_R$  monotonically decreases as the vertical patch size  $L_p$  monotonically increases. The fossil turbulence patch does not collapse, even though the interior turbulent motions monotonically decrease in their vertical extent. Therefore, the patch size  $L_p$  preserves information about the Ozmidov scale  $L_{R0}$  at the beginning of fossilization when the viscous dissipation rate was  $\epsilon_0$ . Thus, from Equation (3) and  $L_{R0} = 0.6 L_R$  we have the expression

$$\epsilon_0 = 0.4 L_p^2 N^3, \quad (7)$$



from which we can estimate  $\omega_0$  from measurements of  $L_P$  and  $N$  long after the turbulence event. Because the saturated internal waves of fossil vorticity turbulence have frequency  $N$ , they propagate vertically, and produce secondary turbulence events above and below the fossil turbulence patch, as shown in the bottom right of Fig. 3. Secondary turbulent events also form on the strong density gradients formed at the top and bottom of the fossil, because these gradient surfaces are likely to be strongly tilted.



**Figure 3.** Fossil turbulence formation on a suddenly tilted density layer in a stagnant stratified fluid. Baroclinic torques cause a buildup of vorticity on the density surface at the top left, causing laminar boundary layers  $v_1$  to  $v_3$ , top center. These become turbulent at 5-10 times the Kolmogorov scale  $L_K$  as shown at top right. Turbulence cascades to larger vertical scales limited by approximately 0.6 times the Ozmidov scale  $L_R$  where fossilization begins, bottom center, leaving a fossil vorticity turbulence remnant, which decays by viscous dissipation and vertical radiation of internal waves that may form secondary turbulence events, bottom right. Microstructure patches are actively turbulent if  $\omega > \omega_0$ , partially fossilized for  $F < F_0$ , and fossil for  $F > F_0$ .

Clearly, to avoid undersampling errors in oceanic microstructure measurements, it is necessary to have a large enough data set for the layer of interest to include many microstructure patches and to examine the hydrodynamic state of those microstructure patches that dominate the average values of the quantities sampled. If the dominant patches are fossilized, then the sample is not representative of the mixing and vertical diffusion processes through the layer. Patches are fossilized if the measured  $\epsilon$  for the patch is less than  $\epsilon_0$  estimated from Equation (7) using the vertical patch size  $L_P$  (maximum Thorpe displacement scale  $L_{Tmax}$ ) and the ambient stratification frequency  $N$  from Equation (4) averaged over scales larger than  $L_P$ . The viscous dissipation rate  $\epsilon$  is defined as

$$2 \epsilon_{ij} e_{ij} ; i,j=1,2,3 ; e_{ij} = \frac{1}{2} \left( \frac{v_i}{x_j} + \frac{v_j}{x_i} \right), \quad (8)$$

where  $e_{ij}$  is the rate of strain tensor and repeated indices implies summation. Dissipation rates  $\epsilon$  can be measured by sampling velocity gradients in the patch at scales of order  $L_K$  or smaller and fitting the measured spectrum to the universal form predicted by Kolmogorov in 1941, or measured directly using Equation (8) assuming local isotropy. It can also be determined by fitting the patch temperature gradient spectrum to the universal spectral form predicted by George Batchelor in 1959 when the wavenumber  $k$  is normalized by the Batchelor scale  $L_B = L_K / Pr^{1/2}$ , where  $Pr = \nu / \kappa$  (10 for the ocean) is the Prandtl number and  $\kappa$  is the thermal diffusivity. Universal velocity and temperature gradient spectral forms, Fig. 1, were first measured by Gibson 1962 using laboratory grid turbulence in water and have since been confirmed in a variety of other flows and fluids.

Motions of the ocean are inhibited in the vertical direction by gravitational forces, so that the turbulence and fossil vorticity turbulence kinetic energy is mostly in the horizontal direction. In Equation (5),  $\Omega_v$  is the vertical component of the Earth's angular velocity and approaches zero at the equator since  $\Omega_v = \Omega \sin \phi$ , where  $\phi$  is the latitude. Large scale winds and currents develop at equatorial latitudes because they are unchecked by Coriolis forces. These break up into horizontal turbulence which can also cascade to large scales before fossilization by Coriolis forces at  $L_H$  scales. Ozmidov and Hopfinger scales for the dominant turbulent events of particular layers, times, and regions of the ocean cover a wide range, with typical maximum values  $L_R = 3-100$  m, and  $L = 30-500$  km occurring where  $\epsilon$  is large and  $N$  and  $\kappa$  are small.

## Quantitative Methods

A patch of temperature, salinity, or density microstructure is classified according to its hydrodynamic state by means of hydrodynamic phase diagrams (HPDs), which compare Froude numbers and Reynolds numbers of the patch to critical values. For the patch to be fully turbulent, both  $Fr$  and  $Re$  must be larger than critical values from the definition of turbulence. If both are subcritical the patch is classified as completely fossilized. Most oceanic microstructure patches are found in an intermediate state, termed partially fossilized, where  $Fr$  is subcritical and  $Re$  is supercritical. This means that the largest turbulent eddies have been converted to saturated internal waves, but smaller scale eddies exist that are still

overturning and fully turbulent. A variety of HPDs have been constructed as fossil turbulence theory has evolved, but all have active, active-fossil, and fully fossil quadrants. Figure 4 shows an HPD introduced by Gibson 1986 applied to turbulence-fossil turbulence-phytoplankton growth interaction.

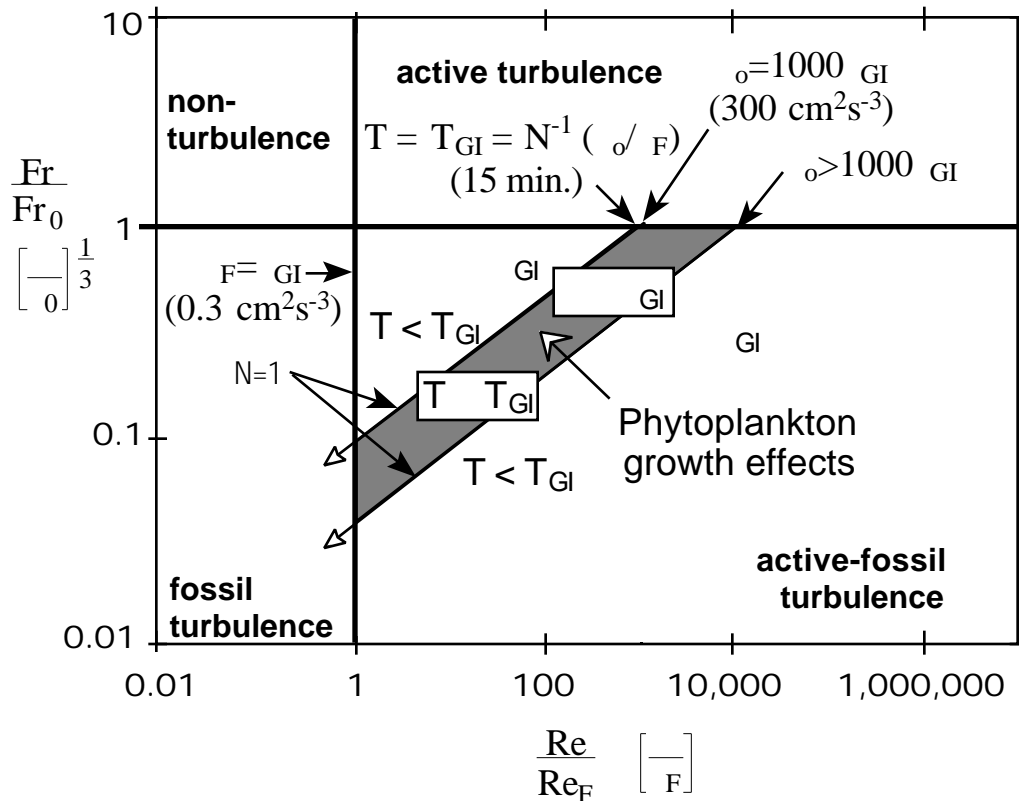


**Fig. 4** Hydrodynamic phase diagram showing the domain of phytoplankton growth effects corresponding to measured values of  $GI = 0.3 \text{ cm}^2 \text{ s}^{-3}$  and  $T_{GI} = 15$  minutes (from Thomas, Tynan and Gibson 1997).

Growth rates of various phytoplankton species are extremely sensitive to both turbulence and the duration of the turbulence. Laboratory experiments reveal that red tide dinoflagellates have two thresholds for growth inhibition; one for turbulence (actually the local strain rate of turbulence since the organism sizes are less than  $L_K$ ), and one for the duration of turbulence to detect fossilization. If the dissipation rate exceeds about  $0.3 \text{ cm}^2 \text{ s}^{-3}$  for more than 15 minutes a day for such microscopic swimmers they die in a few days. Shorter duration turbulence events are ignored, no matter how powerful. Diatom growth in the laboratory and field reacts positively to turbulence events with more than several minutes persistence. The hypothesis matching this behavior is that both classes of species have evolved methods of hydrodynamic pattern recognition so that they can maximize their chances of survival with respect to their swimming abilities.

Dinoflagellate red tides occur when nutrient rich upper layers of the sea experience several days of sun with weak winds and waves so that they become strongly stratified. The diatoms settle out of the light zone so that the dinoflagellates can bloom. However, when waves appear with sufficient strength to mix the surface layer, this is detected by the phytoplankton from the long persistence time of the turbulence fossils the waves produce in the strongly stratified surface layer. The phytoplankton species adjust their growth rates in anticipation of an upcoming sea state change from strongly stratified to well mixed according to their swimming abilities, by hypothesis. The expression relating persistence time  $T = N^{-1} / \epsilon$  to the Reynolds number ratio  $Re/Re_F = \epsilon / \epsilon_F = \epsilon / 30 N^2$  from Gibson 1980 is given at the top of Fig. 4. The gray zone of the HPD permits estimates of the stratification  $N$  and strength of wave breaking turbulence events necessary to inhibit growth of the red tide species studied by both turbulence in the event and the persistence time of the resulting fossil vorticity turbulence.

## Further reading

References are in the Los Alamos E-print archive <http://xxx.lanl.gov>, and in website <http://www-ac.scs.ucsd.edu/~ir118>.

Gibson, C. H., "Fossil Turbulence Revisited", *Journal of Marine Systems*, vol. 21, nos. 1-4, (1999) 147-167, astro-ph/9904237.

Gibson, C. H., "Turbulence in the ocean, atmosphere, galaxy, and universe," *Applied Mechanics Reviews*, 49:5, (1996) 299-315, astro-ph/9904260.

Gibson, C. H., "Kolmogorov Similarity Hypotheses for Scalar Fields: Sampling Intermittent Turbulent Mixing in the Ocean and Galaxy", in *Turbulence and stochastic processes: Kolmogorov's ideas 50 years on*, Proceedings of the Royal Society London, Ser. A, V 434 (N 1890) (1991), 149-164, astro-ph/9904269.